Electronic Supplementary Material (ESI) for ChemComm.
This journal is © The Royal Society of Chemistry 2022

Supporting Information

A Cyclic Organosulfide Cathode with Ultrastable Cycling Performance in Lithium Batteries

*Yao Ren, Yubing Si, Wei Guo, and Yongzhu Fu**

Experimental section

Materials. Toray carbon paper (Fuel Cell Earth, thickness: 190 μm, 0% Teflon coating), liquid carbonate electrolyte (1 M $LiPF_6$ in ethylene carbonate/diethyl carbonate (1:1 v/v), Canrd), lithium bis(trifluoromethanesulfonimide) (LiTFSI, $LiN(CF_3SO_2)_2$, 99.95%, Sigma-Aldrich), lithium nitrate ($LiNO_3$, 99.99%, Canrd), 1,2-dimethoxyethane (DME, 99.99%, Canrd), 1,3-dioxolane (DOL, 99.99%, Canrd), 4,4'-thiodiphenylthiol ($HSC_6H_4SC_6H_4SH$, >98%, TCI), and dimethyl sulfoxide (DMSO, 99%, Macklin) were purchased and used as received. Multiwalled carbon nanotubes (CNTs) were purchased from Nanostructure and Amorphous Materials Inc.

Synthesis of HTBCO and Li_2-TBBT. The synthesis steps for HTBCO are as follows: 50 mg TBBT was added to 200 μL DMSO solution and stirred at room temperature for 12 h. A white solid was obtained and washed with acetone for three times and then heated at 60 °C for 12 h in an oven to remove residual solvent. A white solid was obtained. Li_2-TBBT was synthesized via the reaction between TBBT and lithium foil in DME overnight, followed by volatilizing the solvents.

Preparation of cathode and Li-CP anode. 30 mg HTBCO and 70 mg CNTs were dispersed in 350 mL anhydrous ethanol. They were mixed by ultrasonication, and then the mixture was vacuum filtered onto an 8-cm-diameter filter paper and rinsed with anhydrous ethanol for three times. After being dried in a vacuum oven at 60 °C for 12 h, it was cut into circular discs with a diameter of 12 mm. The active material loading is 1.3 ± 0.1 mg cm^{-2}. The preparation method of the high loading cathode was the same as above, except that the initial HTBCO was 45 mg and the CNTs were 75 mg. To prepare the Li-CP anode, Toray carbon paper (CP) was first cut into circular discs with a diameter of 12 mm and dried in an oven at 100 °C for 24 h. Then the CR2032 coin cells were assembled in an Argon-filled glove box ($H_2O < 0.1$ ppm, $O_2 < 0.1$ ppm).

30 μL of carbonate electrolyte was added into a CP electrode, followed by a Celgard 2400 separator, then another 20 μL electrolyte and lithium anode were added on the separator. The cell was discharged to 0.01 V at 0.025 C on a LAND CT2001A battery test system (Wuhan LAND electronics Co., Ltd, China). Finally, the cell was disassembled inside the glove box and the Li-CP electrode was washed with DME to remove the lithium salt and other substances, and then dried for subsequent use.

Cell fabrication and electrochemical test. CR2032-type coin cells were assembled in the Ar-filled glove box. For the half cells, 20 μL Li-S electrolyte was added to the cathode, and then Celgard 2400 separator was placed on top of the cathode, then another 20 μL Li-S electrolyte and lithium anode were added on the separator. The full cell was assembled the same as above, except the Li foil (diameter: 15.6 mm) was replaced by Li-CP. The Li/HTBCO cell and Li-CP/HTBCO cells were tested between 1.8 and 3.0 V at room temperature. Cyclic voltammetry (CV) was tested by the BioLogic VMP-3. The cell was swept from open circuit voltage (OCV) to 1.9 V and then back to 3 V at 0.1 mV s^{-1}.

Materials characterization. Waters Xevo G2-XS QTof mass spectrometer was used to validate the HTBCO and the cycled products. The cells after cycling were disassembled in the glove box and the cathodes were soaked with DME to obtain the solution of active material. Then they were tested in the atmospheric pressure solids analysis probe (ASAP) positive mode using the first-order mass spectrometry model. Scanning electron microscopy (SEM) imaging of the CP, Li-CP, and Li-CP after 5 cycles at 0.1 C were conducted on a Zeiss Sigma 500 SEM. The elemental distributions of carbon, oxygen, sulfur, and fluorine were analyzed using energy-dispersive X-ray spectroscopy (EDS) attached to the SEM. The X-ray diffraction (XRD) data were collected using a SmartLab SE XRD instrument with Cu Kα radiation. The scanning rate was 2° min^{-1}, and 2θ was set between 10°~70°. The *in situ* XRD test was conducted in a battery mold with a Beryllium window, and the 2θ scan was from 10°~70°. Raman spectroscopy was performed on the Lab RAM HR Evolution Laser Raman spectrometer. Fourier transform infrared (FTIR) spectra were recorded on a Bruker Tensor II infrared spectrometer. X-ray photoelectron spectroscopy (XPS) measurements were conducted with Thermo Scientific K-Alpha.

DFT calculation. The density functional theory (DFT) calculations were performed using

Gaussian 16 program.[1] The global hybrid exchange-correlation functional B3LYP and the "double-ζ" quality def2-SVP basis set were used to conduct structural optimizations and determine harmonic vibrational frequencies. The electrostatic potential (ESP) surface was generated and visualized by Multiwfn program.[2, 3] The coordinates of the optimized HTBCO are shown in Table S1.

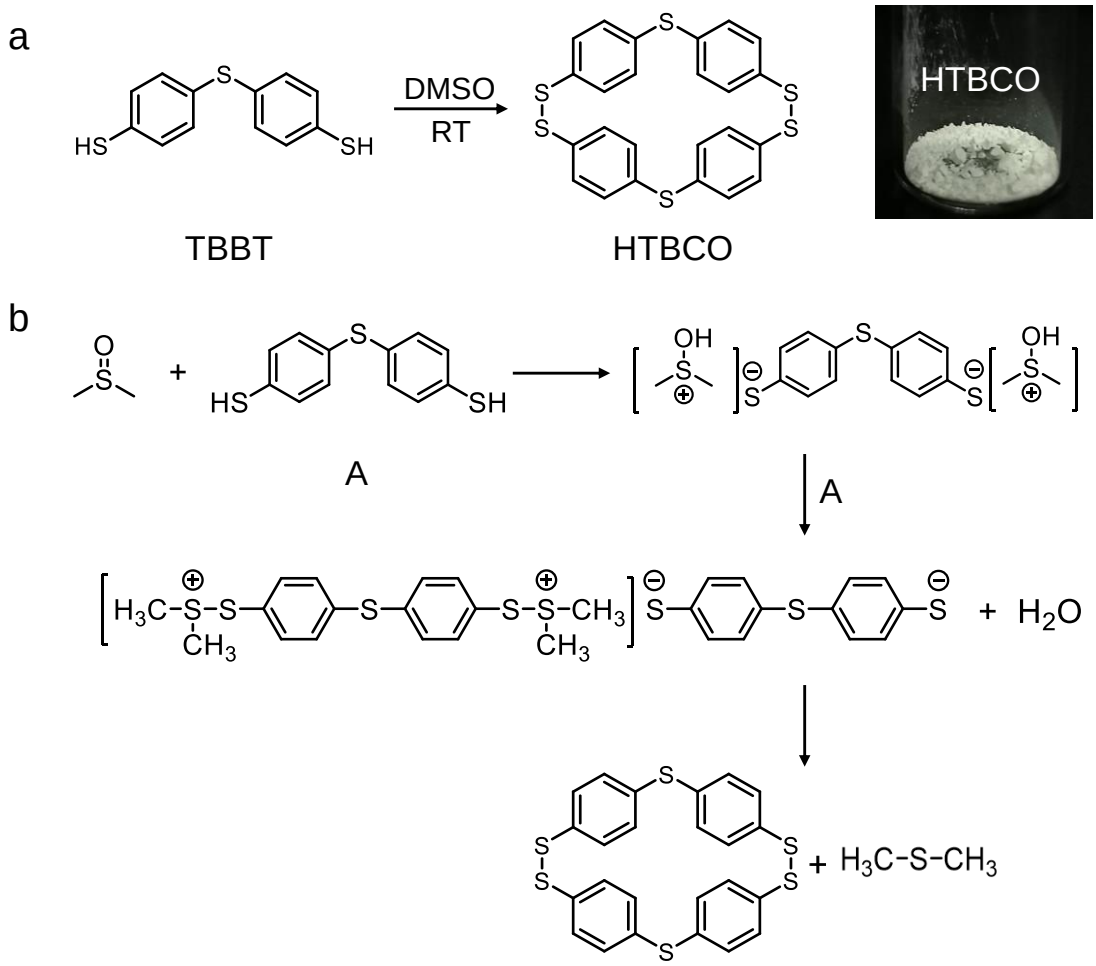

Figure S1. (a) The synthesis process of HTBCO from TBBT. (b) The proposed oxidation mechanism of TBBT.

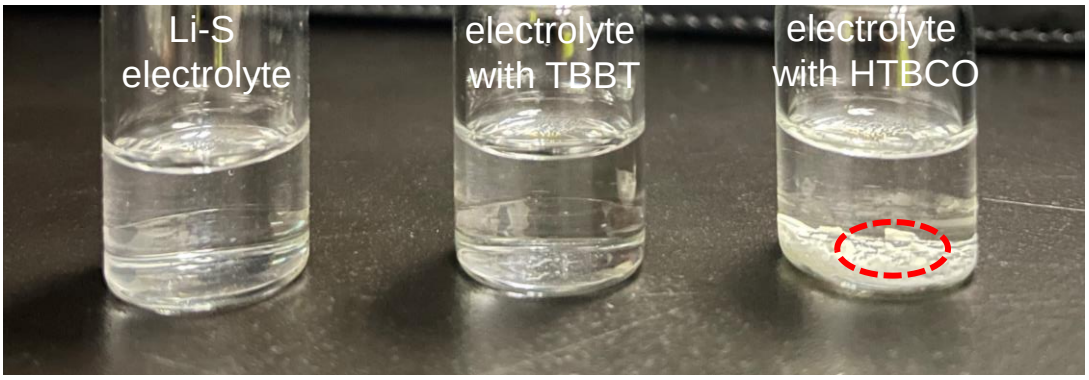

Figure S2. Optical images of the blank Li-S electrolyte and 10 mg TBBT or HTBCO in 2 mL ether electrolyte.

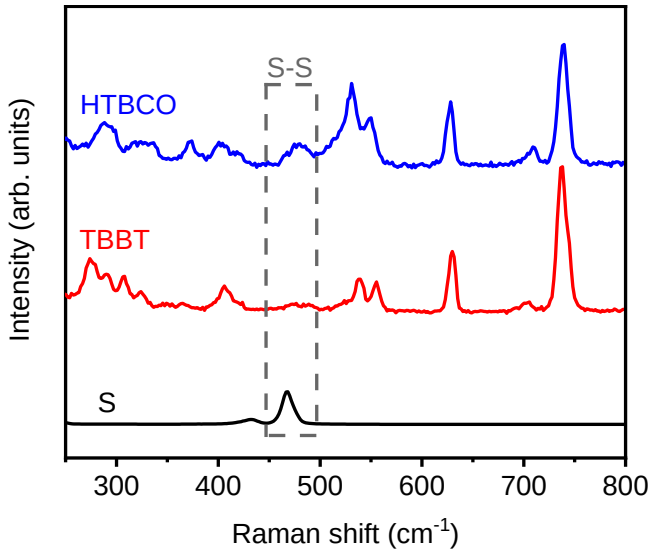

Figure S3. Raman spectra of the S, TBBT, and HTBCO.

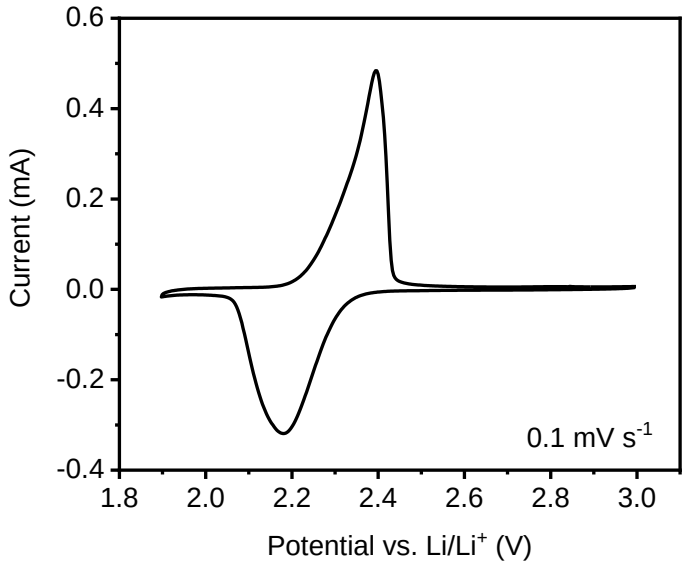

Figure S4. Cyclic voltammogram of the Li/HTBCO cell at a scanning rate of 0.1 mV s^{-1}.

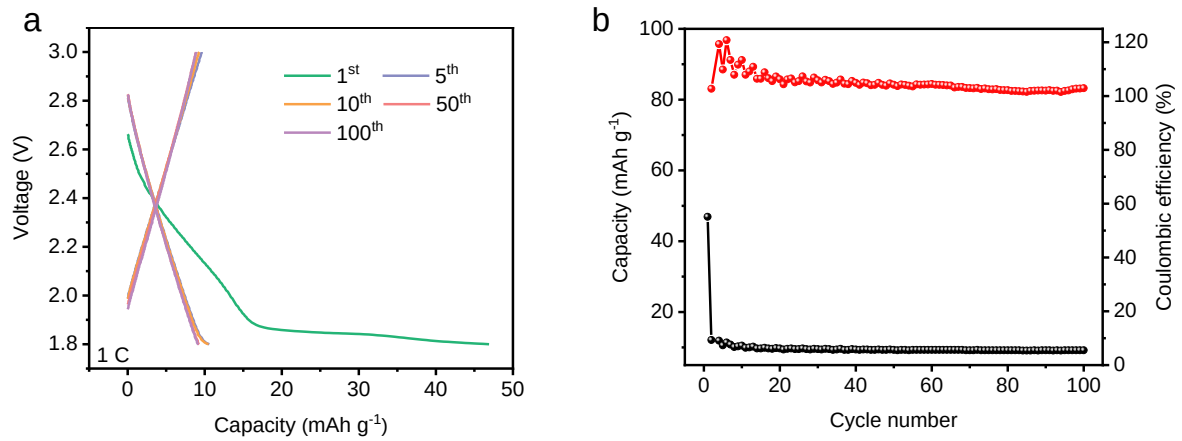

Figure S5. (a) The voltage profiles of the selected cycles of the Li/CNTs cell. (b) Cycling performance of the Li/CNTs cell at 1 C rate.

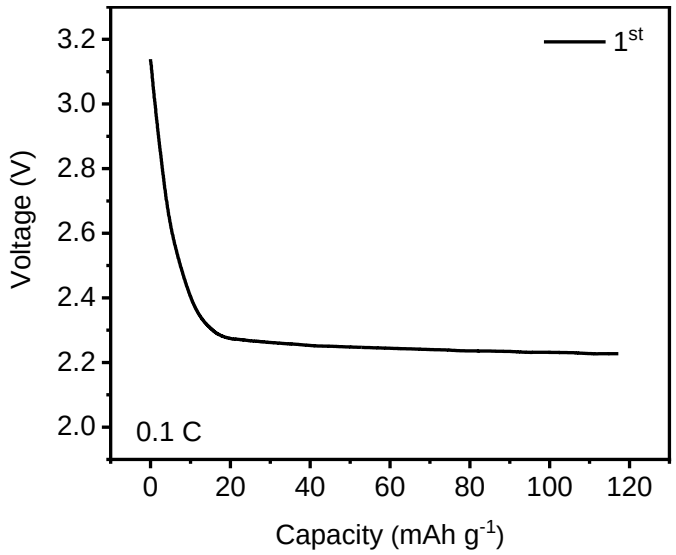

Figure S6. The 1st discharge voltage curve of the Li/HTBCO cell to 0.13 mAh (54.3% depth of discharge) at 0.1 C rate.

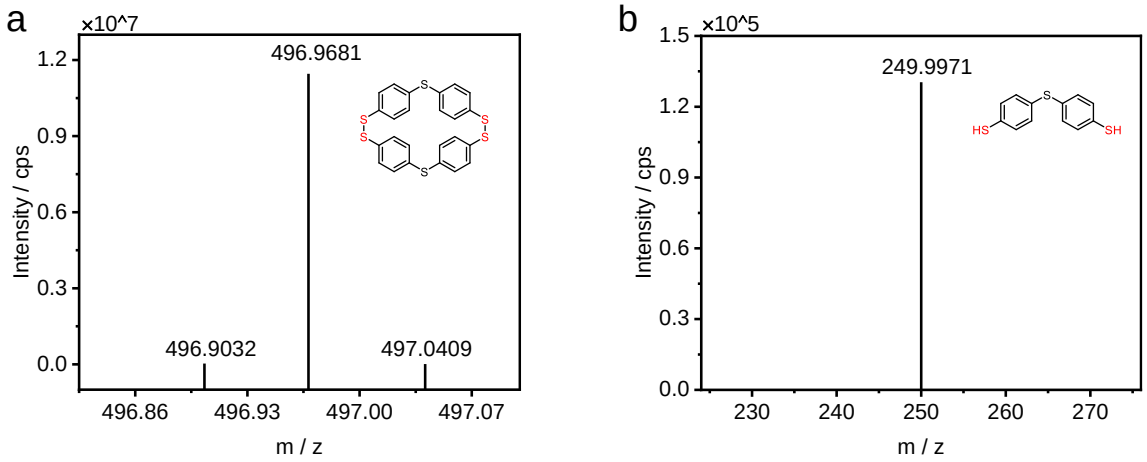

Figure S7. The mass spectra of the recharged/discharged products in the 10th cycle of the Li/HTBCO cell. (a) Recharged product. (b) Discharged product.

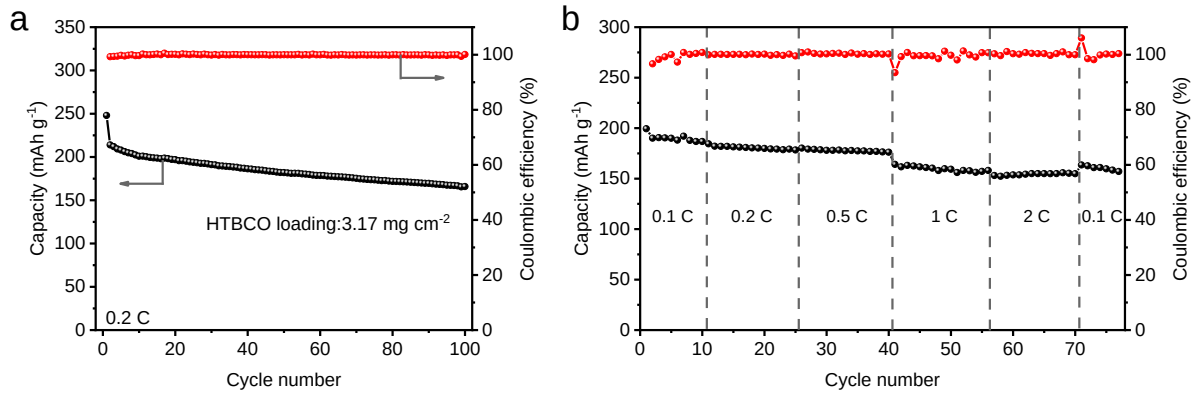

Figure S8. (a) Cycling performance of the Li/HTBCO cell at 0.2 C rate with a mass loading of 3.17 mg cm^{-2}. (b) C-rate performance of the Li/HTBCO cell at 0.1 C, 0.2 C, 0.5 C, 1 C, and 2 C rates and then back to 0.1 C rate.

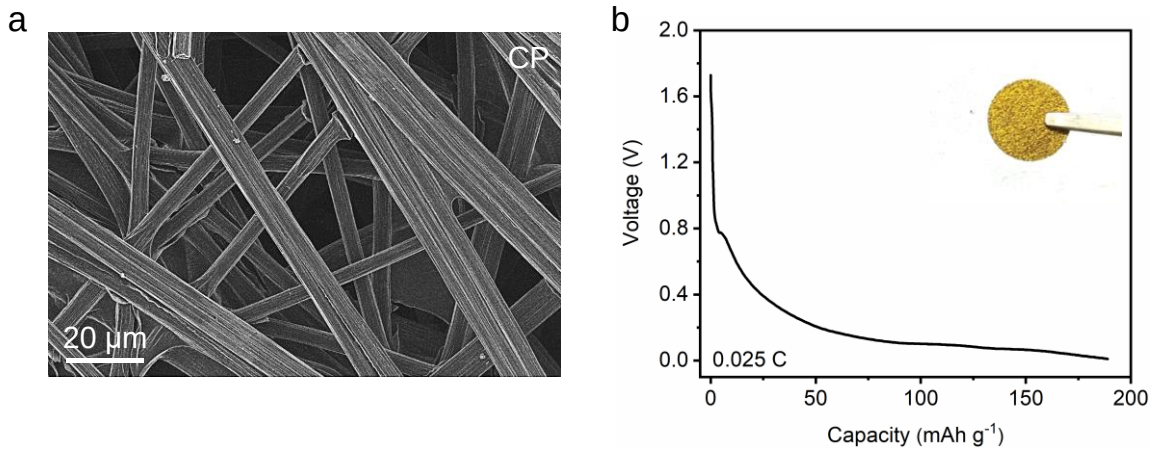

Figure S9. (a) SEM image of the CP. (b) The initial discharge voltage profile of the CP. The inset is a photograph of the lithiated carbon paper (Li-CP).

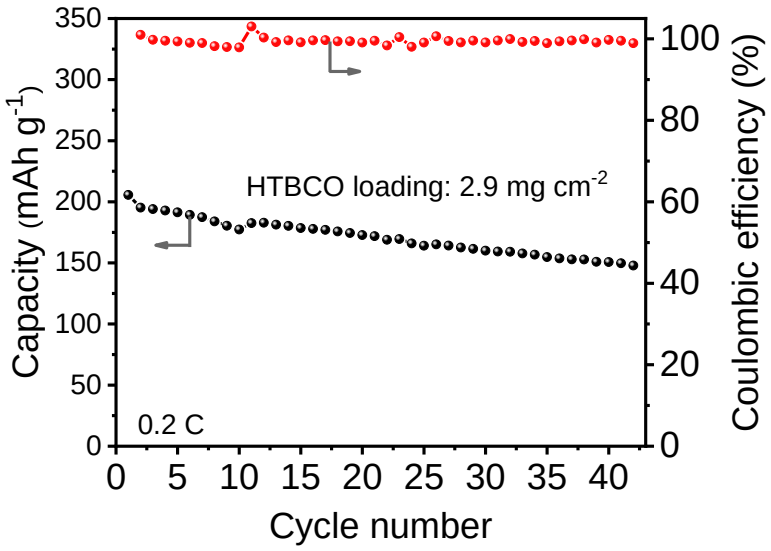

Figure S10. Cycling performance of the Li-CP/HTBCO cell at 0.2 C rate with a mass loading of 2.9 mg cm^{-2}.

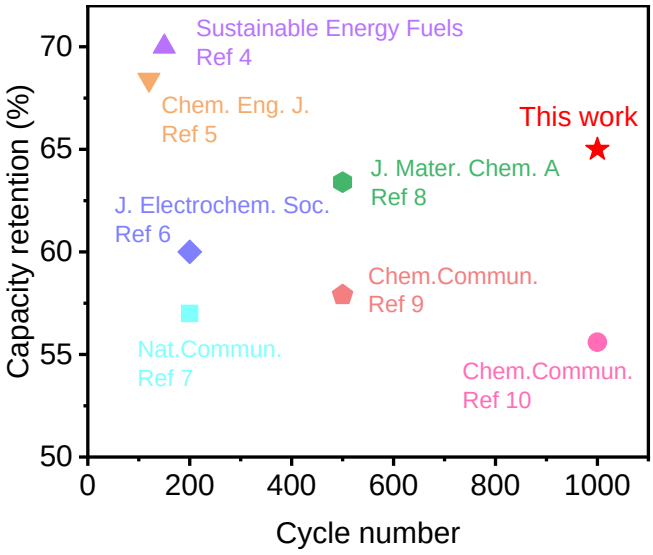

Figure S11. Performance comparison of different organic electrodes.

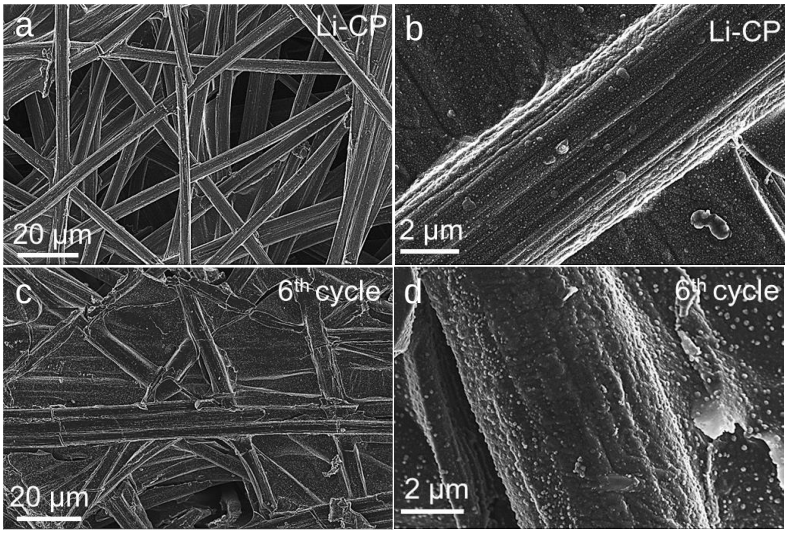

Figure S12. SEM images of the initial Li-CP (a, b) and after 6 cycles (c, d).

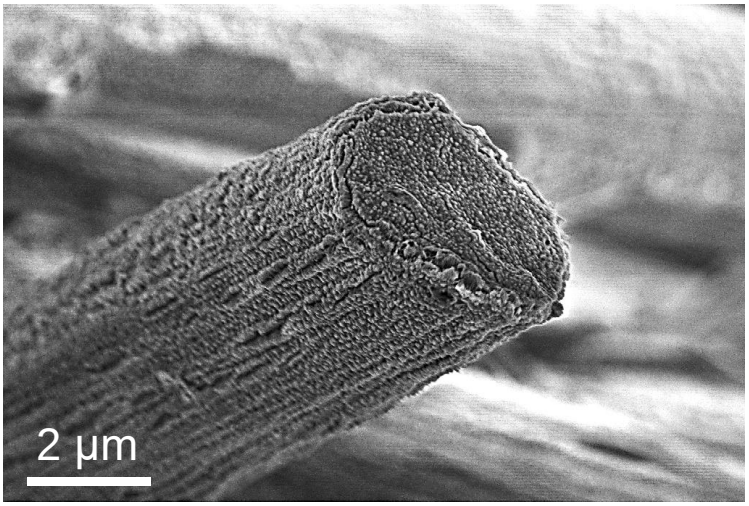

Figure S13. Cross-section SEM image of the Li-CP.

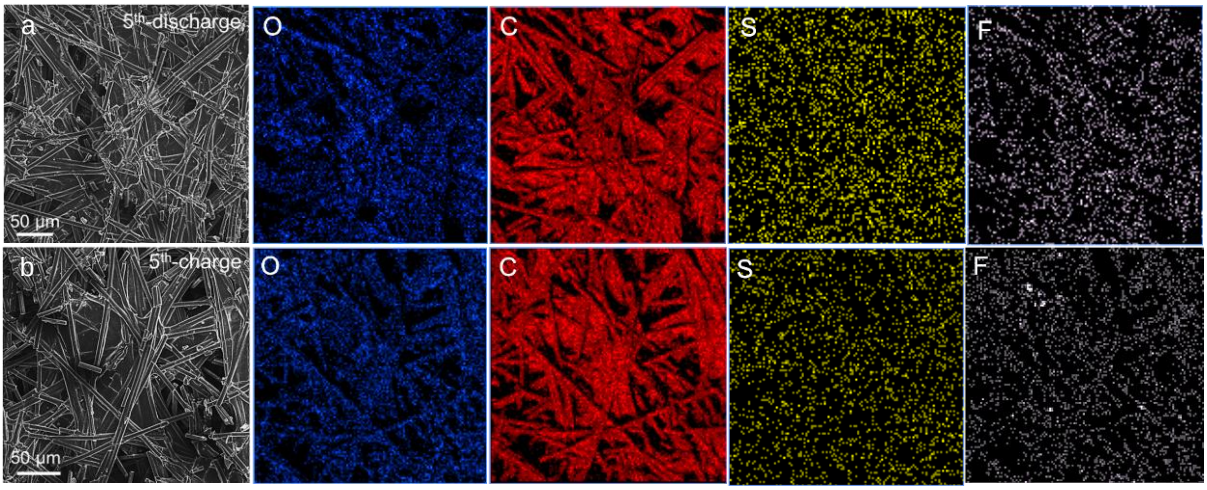

Figure S14. EDS images of the Li-CP anode surface after the 5th cycle in the (a) discharged state. (b) charged state.

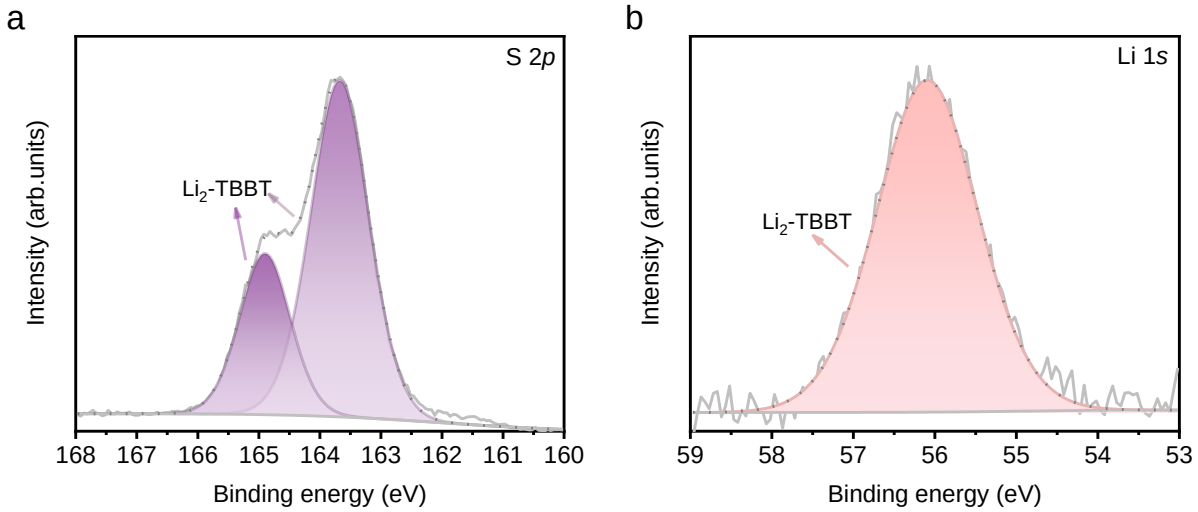

Figure S15. (a) S 2*p* and (b) Li 1*s* XPS spectra of Li_2-TBBT.

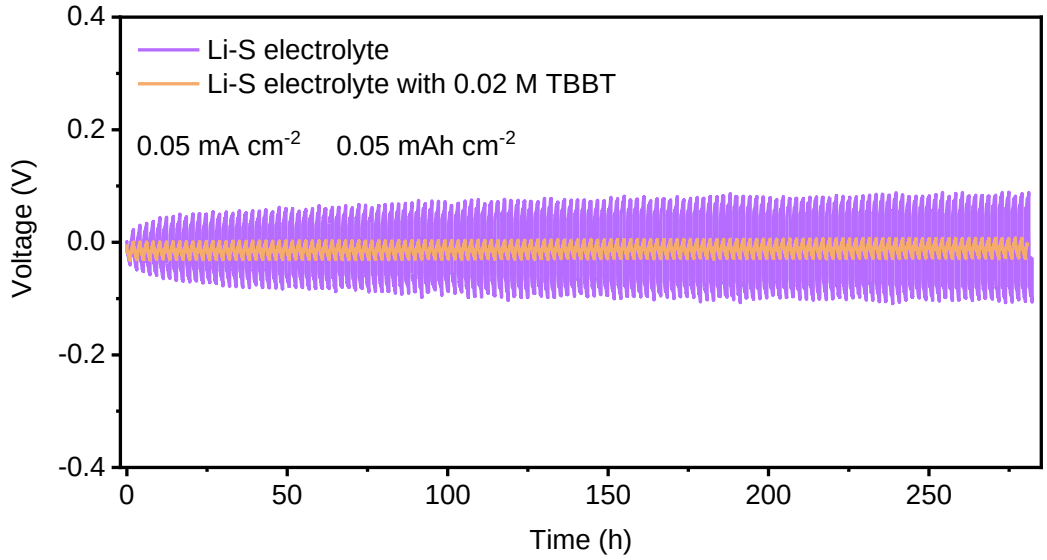

Figure S16. Long-term cycle performance of the Li-CP/Li-CP symmetric cells with TBBT and blank electrolyte.

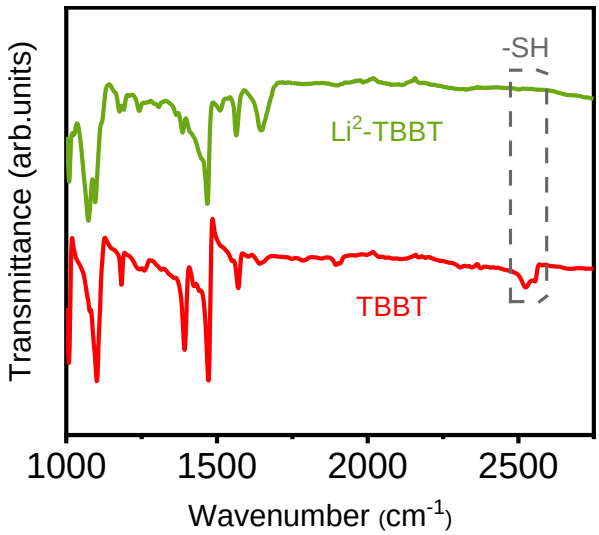

Figure S17. FTIR spectra of the TBBT and Li_2-TBBT.

Table S1. Coordinate of optimized HTBCO.

Element	X	Y	Z
C	-8.12056000	3.18967400	-3.68056000
C	-7.71471000	3.73394300	-4.89961100
C	-6.52203700	3.30384100	-5.50669100
C	-5.74799800	2.31384800	-4.88101600
C	-6.14585700	1.78720400	-3.65292500
C	-7.33196400	2.22185100	-3.03869500
H	-9.04456700	3.53115500	-3.20884000
H	-8.31868400	4.50737200	-5.38032000
H	-4.82879300	1.95966100	-5.35108200
H	-5.53824500	1.02357800	-3.16275900
C	-4.30071400	4.10458200	-6.99350100
C	-3.51502700	3.47927100	-7.97504700
C	-3.67840000	4.84665800	-5.97788000
C	-2.12309600	3.58322700	-7.93372000
H	-3.99929600	2.90449700	-8.76775200
C	-2.28702000	4.92331700	-5.91956400
H	-4.28575500	5.35116500	-5.22350900
C	-1.49878700	4.29055400	-6.89507300
H	-1.51335800	3.09460400	-8.69671200
H	-1.80062700	5.48042800	-5.11600100
S	-7.81749700	1.51131000	-1.47011300

S	0.28410700	4.43563700	-6.79327500
S	-6.08664500	3.99750500	-7.09778100
C	1.20456600	2.98563500	-3.49028100
C	0.80728500	2.91929200	-2.15409200
C	-0.37516100	2.24830600	-1.79820500
C	-1.14808000	1.63565200	-2.79728100
C	-0.76173100	1.72496100	-4.13393400
C	0.41477800	2.40293100	-4.49351700
H	2.12164300	3.51206500	-3.76362400
H	1.41029700	3.40017000	-1.38013700
H	-2.05827900	1.09564200	-2.52977400
H	-1.36986800	1.25839400	-4.91186500
C	-2.58036100	2.36871200	-0.09231800
C	-3.39815900	1.44192300	0.57436000
C	-3.16327600	3.48182300	-0.71784600
C	-4.78301900	1.61874500	0.60330800
H	-2.94538900	0.57599100	1.06278300
C	-4.54862300	3.64080300	-0.71329600
H	-2.53119900	4.21653900	-1.22080300
C	-5.36994600	2.70966400	-0.05581800
H	-5.41792700	0.89519100	1.11915000
H	-5.00500500	4.49525200	-1.21742700
S	0.88732200	2.47841800	-6.21822300

S	-7.14347200	2.95961400	-0.06124500
S	-0.80332500	2.14222100	-0.06364200

References:

1. M. J. Frisch, G. W. Trucks, H. B. Schlegel, G. E. Scuseria, M. A. Robb, J. R. Cheeseman, G. Scalmani, V. Barone, B. Mennucci and G. A. Petersson, 2016, DOI: 10.1039/c7ta07460c.
2. T. Lu and F. Chen, *J. Comput. Chem.*, 2012, **33**, 580−592.
3. J. Zhang and T. Lu, *Phys. Chem. Chem. Phys.*, 2021, **23**, 20323−20328.
4. A. Bhargav, S. V. Patil and Y. Fu, *Sustainable Energy Fuels*, 2017, **1**, 1007−1012.
5. P. Sang, J. Song, W. Guo and Y. Fu, *Chem. Eng. J.*, 2021, **415**, 129043.
6. C. Xing, P. Xue, X. Gu and C. Lai, *J. Electrochem. Soc.*, 2018, **165**, A3782−A3784.
7. D. Y. Wang, Y. Si, W. Guo and Y. Fu, *Nat. Commun.*, 2021, **12**, 3220.
8. F. Li, Y. Si, Z. Li, W. Guo and Y. Fu, *J. Mater. Chem. A*, 2020, **8**, 87−90.
9. P. Sang, Y. Si and Y. Fu, *Chem. Commun.*, 2019, **55**, 4857−4860.
10. Q. Pan, J. Lan, Y. Si, W. Guo and Y. Fu, *Chem. Commun.*, 2022, **58**, 5602−5605.